Algerian Journal of Engineering and Technology

Journal homepage: https://jetjournal.org/index.php/ajet

Original Article

Adsorptive, kinetic and thermodynamic investigations of *Sarcocephalus latifolius* leaves extract as corrosion inhibitor on alloy steel in 0.6M HCl solution

Fater Iorhuna and Abdullahi Muhammad Ayuba*

Department of Pure and Industrial Chemistry, Faculty of Physical Sciences, Bayero University, Kano, Nigeria

ARTICLE INFO

Article history:
Received 18 October 2022
Revised 18 November 2022
Accepted 19 November 2022

Keywords:
Alloy steel;
Sarcocephalus latifolius;
Pysisorption;
Freundlich isotherm;
First order kinetics.

ABSTRACT

One of the materials that have many uses in the manufacturing, automotive, and construction industries is the alloy steel. When exposed to harsh environments this material is susceptible to deterioration and corrosion. Because of this reason, it is necessary to safeguard this valuable material. There have been many different methods used, but inhibition using particularly plant extract has reportedly been effective and acceptable to the environment. In this study, the behavior of alloy steel in 0.6M HCl at various concentrations of *Sarcocephalus latifolius* extract was assessed using weight loss and surface characterization methods of analysis. The plant extract's ability to inhibit corrosion increased during the weight loss experiment from 25.56% to 61.18% as concentration of the plant extract increased with a decrease in temperature from 323K to 303K respectively. Thermodynamic parameters of the inhibitory process were discovered to classify the process as feasible and spontaneous, obeying the Freundlich adsorption isotherm model's description of physical adsorption. The kinetic analysis of the inhibitory process demonstrates that it follows the first order model, with activation energy and half-life values rising with the concentration of the plant extract. In conclusion, *Sarcocephalus latifolius* extract is effective in inhibiting the corrosion of alloy steel in 0.6M HCl at low temperatures and higher plant extract concentrations through surface adsorption.

1. Introduction

The building of equipment used in various environments such as agriculture, oil and gas, petrochemical, automobile and allied sectors as well as in medical laboratories heavily relies on metallic materials made of zinc, aluminum, iron and their alloys. Due to corrosion activities on their surface, metallic materials in harsh environments gradually lose property, luster, function, and ability over time as a result of daily interactions with their immediate environment [1]. The majority of reactive metals are known to exist naturally in combined forms; these metals typically resist being transformed into pure forms during purification processes. After isolation and purification, they tend to frequently return to their natural combined form, which is thermodynamically more stable [2].

Corrosion is the gradual loss of a material's chemical and physical properties caused by environmental factors like air and moisture, which typically affects the materials [2]. Naturally, corrosion can occur on a variety of materials, but metals have historically been the most frequently affected [3]. Corrosion may be caused by chemical cleaning, pickling and rescaling of the metals in industries using acids at low concentration (ie 0.6M HCl) [2]. To lessen the issues caused by this harmful phenomenon known as corrosion, such as the cost of production, repair, replacement, accidents, and health related issues associated therewith, numerous methods of prevention or controlling the menace of corrosion have been developed by scientists worldwide [4]. One of the most efficient and cheap ways to stop metals from corroding is to utilize inhibitors that

* *Corresponding author*. Tel.: +2348062771500
E-mail address: ayubaabdullahi@buk.edu.ng
Peer review under responsibility of University of El Oued.
2716-9227/© 2022 The Authors. Published by University of El Oued. This is an open access article under the CC BY-NC license (https://creativecommons.org/licenses/by-nc/4.0/).

contain heteroatoms. Scientists once thought that chromates served as a protective barrier for metals in corrosive conditions. Environmental specialists, however, advised against using it because of its level of toxicity [5-6]. In order to address the issues of harmful inhibitors degrading the environment, research is increasingly focusing on environmentally benign inhibitors including the utilization of plant materials [7-9].

A good adsorptive capacity is attributed to plant extracts that contain phytochemicals with diverse functional groups, heteroatoms, or polar atoms like sulphur (S), nitrogen (N), oxygen (O), or phosphorus (P) due to the presence of lone pair of electrons on them. As a result, corrosion-causing oxide is prevented from forming when metallic materials lose electrons from their d-orbitals. According to certain mechanisms, the phytochemicals in plant extract form a connection with the metal surface and stop corrosion in its surface holes and tracks [10].

The objective of the current study is to use different concentrations of the plant extract in low concentration of acid (0.6M HCl) at various temperatures as a corrosion inhibitor on alloy steel surfaces. This is planned to be achieved by using surface characterization techniques and weight loss experiments. To the best of our knowledge, the plant (*Sarcocephalus latifolius*) leaves has not been reported in literature for use in corrosion inhibition studies.

2. Materials and Methods

2.1. Preparation of Alloy Steel Specimens for Test

The alloy steel used for this experiment is made up of the components reported in Table 1 and the composition was obtained through the use of energy-dispersive x-ray fluorescence (XRF) technique. The sheets were mechanically press-cut into coupons that were 4cm x 3cm x 0.5cm in size. The coupons were then polished with different grades of Silica carbide abrasive paper (#400 to #1200). The polished coupons were cleaned with distilled water, ethanol, dried in acetone and stored in an airtight desiccator for further use [11].

Table 1. Composition of the alloy steel determined through XRF method

Element	Composition (%)
Fe	81.37
Na	9.30
Al	5.76
Zn	2.48
Si	0.40
Mn	0.27
Nd	0.16
Cr	0.08
Ti	0.07
C	0.11

2.2. Collection, Preparation and Extraction of the Plant Sample

The samples of *Sarcocephalus latifolius* leaves were obtained from the Iorhuna Uyer Farm yard in the village of Apkuuna (1), Mbapenda local government area, Mbazum Mbaterem Ukum, Benue State, Nigeria. A certified botanist identified the leaves samples before they were washed and dried under shed, ground with a metal mortar and pestle, and sieved through 75µm mesh. *Sarcocephalus latifolius* leaves powder sample weighing 500g was soaked in 2.5 liters of 95% methanol for two (2) weeks with continuous stirring. Whatmann No. 1 filter paper was used to filter the mixture after percolation. The extract was concentrated using rotatory evaporator (BUCHI labortechnik AG/9230 flawil/Switzerland) and thick syrup was obtained. The thick syrup was then air dried until a constant weight was obtained at room temperature. The dried extract was further crushed using a mortar and pestle to increase its surface area and hasten its dissolution in the corrosive 0.6M HCl solution [12].

2.3. Preparation of Corrodent Solution

0.6M HCl solution serving as the corrodent was prepared using equation 1,

$$V_{stock}\,(ml) = \frac{M \times C \times V}{10 \times \%purity \times density} \quad (1)$$

Where M is molar mass of the corrodent, C is the final concentration of the corrodent (0.6M), V is the final volume of the solution, V_{stock} is the volume of the concentrated HCl before dilution, % purity and density of HCl [13-14].

2.4. Weight Loss Measurements

TOLEDO Mettler analytical weighing balance was used to weigh the alloy steel coupon samples before and after immersion in the corroding liquid with or without the plant extract. 100cm^3 of the various test solutions containing 0.0, 0.2, 0.4, and 0.6g/L of the plant extract in 0.6 M HCl solution where prepared in a beaker. The weighed alloy steel coupon was submerged entirely in the prepared solution differently. The 0.0g/L solution containing only 0.6M HCl was used as the control. The beakers containing the samples were placed in a vacuum thermostatic water bath whose temperatures where set at 303K, 313K and 323K. The experiment was run for a total period of 4 hours and the immersed test coupons were retrieved out of the corroded media at 1 hour intervals. Each retrieved coupon was then washed in distilled water using a plastic brush, dried in acetone and reweighed. The percentage inhibition efficiency, surface coverage and corrosion rate were determined using equations 2-4 and values derived from the difference in weights of the alloy steel coupon for the

inhibited and uninhibited experiment where used for the calculations [15-16].

$$\%I.E. = (1 - \frac{W_i}{W_f}) \times 100 \quad (2)$$

$$\theta = 1 - \frac{W_i}{W_f} \quad (3)$$

$$CR(\frac{g}{hcm^2}) = \frac{\Delta W}{At} \quad (4)$$

Where (θ) is the degree of surface coverage, (CR) is the corrosion rate, (Δw) is the weight loss in (g), A is the area of the metal coupon (cm^2), (t) is the immersion time in hours (h), and w_i and w_f are the weight loss in grams (g) of alloy steel in the absence and presence of inhibitor, respectively.

2.5. Fourier Transform Infrared (FT-IR) Analysis

FTIR instrument model: Cary 630 FTIR Spectrophotometer (Agilent Technologies), was used to identify the principal functional groups found in the samples of *Sarcocephalus latifolius* leaves extract and that of the alloy steel coupon that had been inhibited in solution containing 0.6g/L of the plant extract in 0.6M HCl at room temperature. Prior to analysis, the studied coupon was submerged for a period of 4 hours in $100cm^3$ of the test solution. A maximum of 32 scans were performed on the materials during the study, which covered the wave number range of 650-4000cm^{-1} at 8cm^{-1} resolution [17-18].

2.6. Scanning Electron Microscopy

Using a Prox Scanning Electron Microscope (Phenom World Eindhoven), the coupons' surface morphology for the inhibited and uninhibited alloy steel was examined. Before analysis, the coupons were placed in solutions of 0.6M HCl containing the leaves extract of *Sarcocephalus Latifolius* and allowed to stay for 1 week at 303K. During sample preparation, a very little amount of the materials to be scanned was placed on the stub materials and afterwards observed in the 1000x magnification. The scanned micrographs were captured at a 15.00kV accelerating voltage.

3. Results and Discussion

3.1 Weight Loss

Table 2 reports the weight loss experimental findings of *Sarcocephalus latifolius* extract's corrosion inhibition on alloy steel in 0.6M HCl. The findings are obtained by the following experimental conditions: temperatures between 303K and 323K were varied in a series with a common difference of 10K at various inhibitor concentrations of 0.2g/L, 0.4g/L and 0.6g/L in an aqueous environment with 0.6 M HCl. According to the findings, the corrosion rate decreases when the plant extract concentration rises from 0.2g/L to 0.6g/L, as shown in Table 2. At the highest plant extract concentration of 0.6g/L, the corrosion inhibition increases from 44.99% to 61.18% as the temperature falls from 323K to 303K. This demonstrates the plant extract's efficacy on the surface of alloy steel. Comparing the corrosion rate of the coupons with respect to a given plant extract concentration with rises in temperature, the rate of corrosion was found to increases, which demonstrates that, as temperature rises, the alloy steel's surface is more subjected to corrosion and the plant extract become less effective. Also as the system's temperature rises, the inhibition efficiency (IE) of the plant extract on the metal's surface decreases. Therefore, the inhibitory potency of the extract of *Sarcocephalus latifolius* becomes more effective at increasing concentration and lower temperature [12, 15-18].

Table 2. Parameters of weight loss experiment determined

Temp (K)	Extract Conc. (g/L)	Δw (g)	CR (g/cm^2.h) $x10^{-4}$	θ	IE. (%)
	0.0	0.0121	2.52	-	-
	0.2	0.0067	1.40	0.4463	44.63
303	0.4	0.0058	1.21	0.5207	52.07
	0.6	0.0047	0.98	0.6118	61.18
	0.0	0.0271	5.65	-	-
	0.2	0.0197	4.10	0.2731	27.31
313	0.4	0.0182	3.79	0.3284	32.84
	0.6	0.0143	2.98	0.4723	47.23
	0.0	0.0489	0.10	-	-
	0.2	0.0364	7.58	0.2556	25.56
323	0.4	0.0341	7.10	0.3027	30.27
	0.6	0.0369	5.60	0.4499	44.99

3.2 Fourier Transform Infrared Spectroscopic (FTIR) Analysis

The functional groups present in the methanol extract of *Sarcocephalus latifolius* as well as the corrosion-preventing film generated on the surface of the alloy steel were identified using FTIR analysis. Figure 1a displays the FTIR spectrum of the methanol leaves extract of *Sarcocephalus latifolius*, while Figure 1b displays the spectrum of the corrosion product. From the wavenumbers presented in Table 3, the absorption bands of the two spectra for the plant extract and corrosion product were compared, the positions of the bands were seen remain unchanged for the following functional groups: Alkyne (C≡C), Acid (RCOOH) and Nitrosamine (RN-N=O). The shift in the values of some wavenumbers where observed for some functional groups which include: from 2921 to 2925cm^{-1} for the C-H stretching, from 3301 to 3316cm^{-1} for N-H stretching, 1108 to 1074cm^{-1} for C-O

stretching,1030 to 1037cm^{-1} for polysaccharides, 1603 to 1622cm^{-1} for N-H bending and 1194 to 1201cm^{-1} for C-N stretching. O-H stretching with a wavenumber of 3692cm^{-1} was observed in the *Sarcocephalus latifolius* leaves but absent in the corrosion product. The adsorption of various elements of the methanol extract from *Sarcocephalus latifolius* leaves on the metallic surface is indicated by the aforementioned alterations in absorption bands. According to the surface examination performed using FTIR, the plant extract may contain functional groups such as hydroxyl (-OH), carboxylic acid (-COOH), methylene (-C≡C-), amine (-N-H), cyanides (-C-N), nitrosamine (-N-N=O) and carbonyl groups (C=O) from polysacharides. The interaction of the plant extract with the alloy steel surface must have been facilitated as a result of the phytochemicals present there-in that contain the above mention functional groups [13-14, 19].

Table 3. Summary of FTIR absorption bands of the samples studied

Functional group	**Absorption location (cm^{-1})**	**Methanol Extract (cm^{-1})**	**Inhibited Metal (cm^{-1})**	**Difference (cm^{-1})**
Alkane (C-H)	2850-2975	2921, 2854	2925, 2854	-4
Alcohol(O-H)	3400-3700	3692	-	3692
Alkyne (C≡C)	2100-2250	2119	2119	0
Amines (N-H)	3300-3350	3301	3316	-15
Acid (RCOOH)	1700-1725	1707	1707	0
C-O stretch	1000-1320	1108	1074	34
Nitrosamine	1440-1470	1443	1443	0
Polysaccharides	1030-1149	1030	1037	-7
N-H bend	1580-1650	1603	1622	-19
C-N stretch	1020-1250	1194	1201	-7

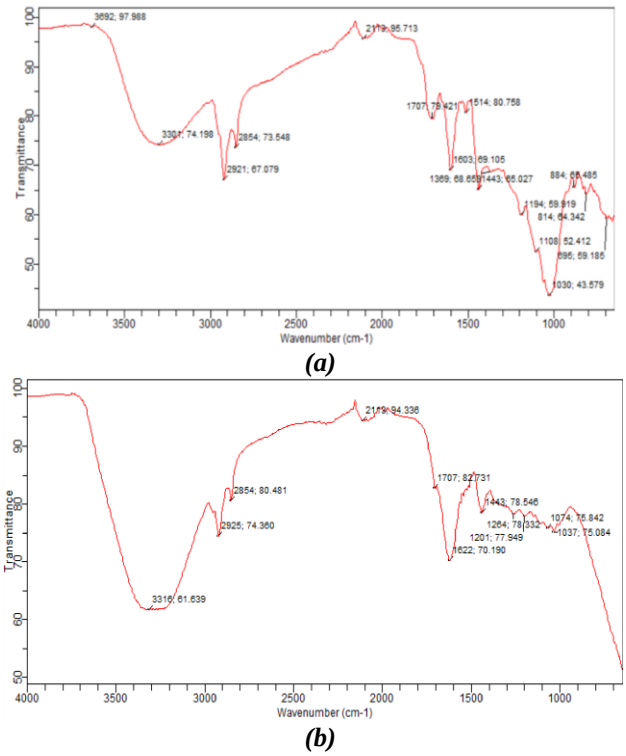

Fig 1. FTIR spectra of (a) methanol leave extract of *Sarcocephalus latifolius*, (b) corrosion product of alloy steel immersed in 0.6M HCl containing methanol leave extract of *Sarcocephalus latifolius*.

3.3 Scanning Electron Microscopy (SEM) Analysis

Utilizing scanning electron microscopy, it was possible to compare the surface morphology of alloy steel with and without inhibition of the plant extract. When the coupons were dipped in solution of 0.6M HCl with and without the plant extract for 1 week at room temperature, SEM images of magnification 1000x were captured using an electron probe micro analyzer [6]. The outcomes are shown in Figure 2. Figure 2a depicts the surface of alloy steel before corrosion. Figure 2b depicts the same alloy steel in a blank solution containing 0.6M HCl characterized with a rough, broken, and ruptured surface. The plant extract, however, was able to cover the surface of the coupons with an increasing amount of effect as the plant extract concentration increased from 0.2g/L to 0.6g/L when the alloy steel samples were placed in various concentrations of the plant extract (see Figure 2c for 0.2g/L, Figure 2d for 0.4g/L, and Figure 2e for 0.6g/L inhibited systems). The images in Figures 2c–e showed that the extract of *Sarcocephalus latifolius* leaves in 0.6M HCl had covered the rough and rupture surface of the alloy steel surface reducing the rough surface with increase in plant extract concentration.

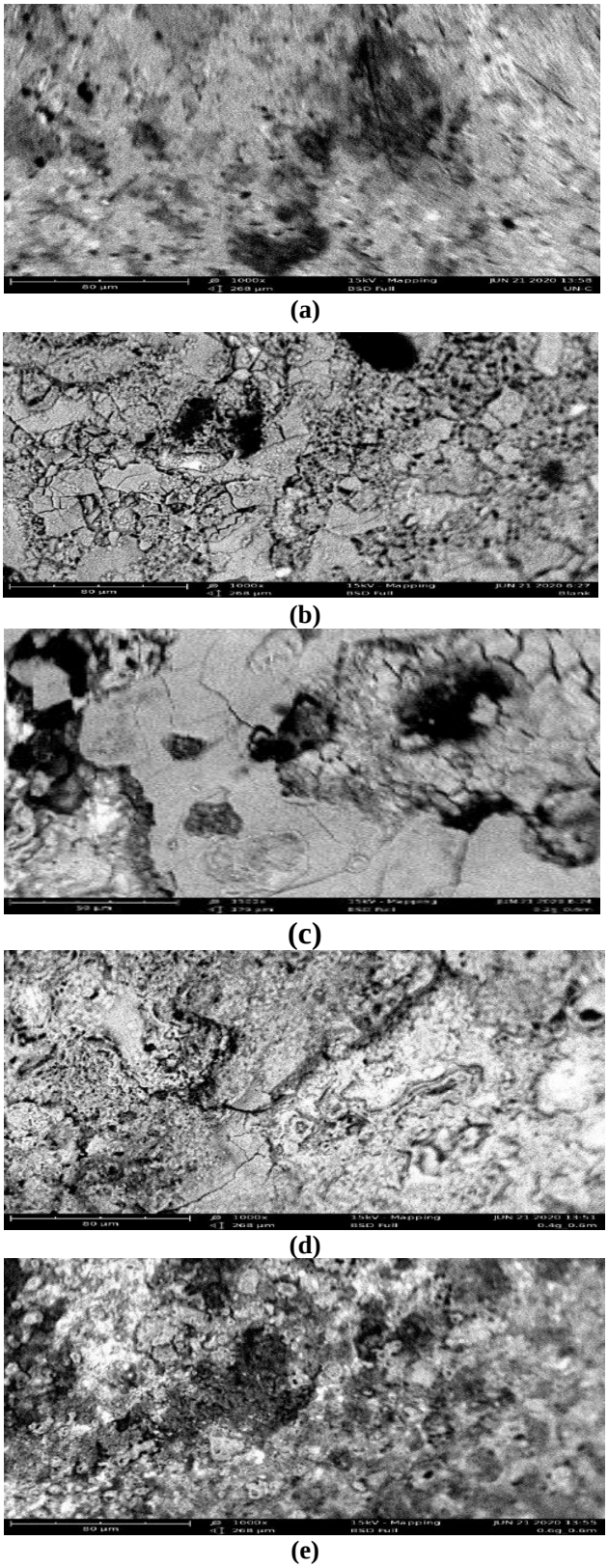

Fig 2. SEM micrographs of (a) un-corroded alloy steel (b) alloy steel in 0.6M HCl (c) in 0.2g/L (d) in 0.4g/L (e) in 0.6g/L plant extract

3.4 Adsorption Isotherms

The ability of inhibitors to bind to metal surfaces determines how effective they are during the process of inhibition. The nature of corrosion inhibitors has been determined in terms of adsorption characteristics, which prevents corrosion and metal degradation [14]. Surface coverage (θ) and inhibitor concentration can be used to achieve this phenomenon. Inhibitors adhere to the surface of metals to produce an adsorptive coating, which prevents corrosion. Many isotherm models, some of which are listed Table 4 where being employed in this experiment, describe the nature and effectiveness of the coverage of inhibitors on the surface of metals. It is believed that the components of the *Sarcocephalus latofolius* leaves extract adsorb onto the surface of alloy steel, creating a layer of protection against the corrosive acid environment and inhibiting the corrosion process [20–23]. Data collected from the degree of surface coverage (θ) of this kind is typically fitted into several adsorption models developed by Temkin, Langmuir, Freundlich, Florry-Huggins and El-Awady in order to adequately describe the mechanism of adsorption and nature of the surface complex created. In this work, the Langmuir and Freundlich isotherm models, two of the most well-known of them, were selected and employed. Since each of these isotherms abides by the same formula, equation 5 can generally be used to represent all of them.

$$f(\theta, x)exp^{(-2a\theta)} = K_{ads}C_{inh} \quad (5)$$

Where x is the size ratio, 'a' is the lateral molecule interaction parameter, and K_{ads} is the equilibrium constant of adsorption, f(θ, x) denotes the configuration factor, which depends on the physical model and assumptions underpinning the isotherm's derivation [4]. The formulae for the Langmuir and Freundlich adsorption isotherms are shown in Table 4 in their various forms.

Table 4. Forms of Langmuir and Freundlich adsorption isotherms

Isotherm	Conversional Form	Linear Form
Freundlich	$\theta = K_{ads}(C_{inh})^{n}$	$\ln\theta = n\ln C_{inh} + \ln K_{ads}$
Langmuir	$\theta/(1-\theta) = K_{ads}C_{inh}$	$C_{inh}/\theta = 1/K_{ads} + C_{inh}$

Where θ is the degree of surface coverage of the inhibitor, K_{ads} is the equilibrium constant of adsorption, Cinh is the concentration of the inhibitor and n is the interaction parameter.

The production of monolayer adsorbate on the surface of the adsorbent was quantitatively represented using the Langmuir adsorption isotherm. The model presupposes homogeneous adsorption energies on the surface and a lack of adsorbate transmigration in the surface plane [13]. The findings of a C_{inh}/θ versus C_{inh} plot are shown in Figure 3.

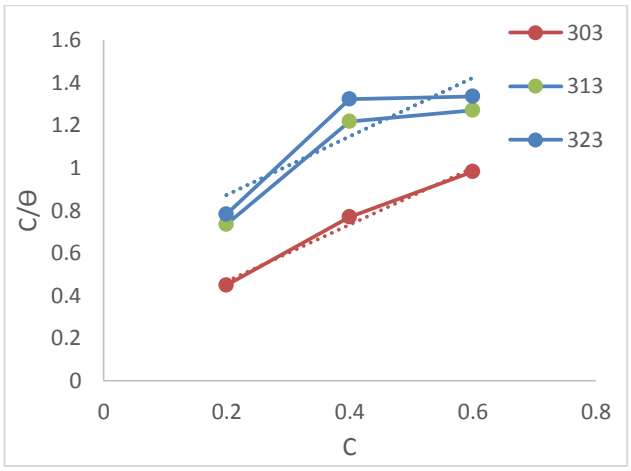

Fig 3. Langmuir isotherm for *Sarcocephalus latifolius* extracts on the surface of alloy steel in 0.6M HCl solution at various temperatures

Figure 4 illustrates the straight line obtained from the plot of lnθ versus lnC for Freundlich isotherm, which has a slope of n and an intercept of lnK_{ads}. When compared to the Langmuir data in terms of the value of R^2, which is closer to unity than other isotherms, the data analyzed relatively follows the Freundlich isotherm model. The interaction intensity in the adsorbed layer is indicated by the adsorption equilibrium constant, K_{ads}, and the constant 'n,' where $0 \leq n \leq 1$.

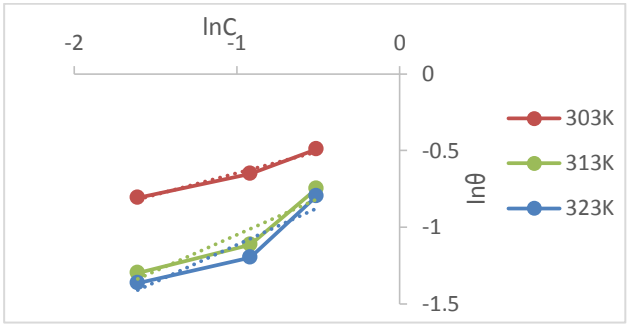

Fig 4. Freundlich isotherm for *Sarcocephalus latifolius* leaves extract on the surface of alloy steel in 0.6 HCl solutions at various temperatures

The extracts' adsorbed components interact significantly and strongly, and the interaction is independent of all variables other than temperature, according to positive and large values of K_{ads} provided in Table 5. It can be seen that K_{ads} drops as the temperature rises, indicating a decrease in the adsorption strength of these components. Equation 6 representation of the direct relationship between adsorption ΔG_{ads} and K_{ads} at a specific temperature (T) was utilized to determine ΔG_{ads} for the adsorption of *Sarcocephalus latifolius* extract onto alloy steel surface.

Table 5. Calculated values of parameters for the tested isotherms models

Isotherm	Temp. (K)	Slope	ΔG_{ads} ($kJmol^{-1}$)	R^2	K_{ads}
Langmuir	303	1.33	-14.181	0.9867	5.01
	313	1.34	-12.079	0.8222	1.87
	323	1.38	-12.184	0.7663	1.68
Freundlich	303	0.28	-9.195	0.9738	0.69
	313	0.47	-8.959	0.8911	0.56
	323	0.49	-9.102	0.8635	0.53

3.4 Thermodynamic Studies

The free energy of adsorption, ΔG_{ads} was calculated according to equation 6

$$\Delta G_{ads} = -2.303RTlog(55.5K_{ads}) \quad (6)$$

Where ΔG_{ads} is the change in the Gibbs free energy of adsorption, K_{ads} is the equilibrium constant for adsorption determined from the intercept of each adsorption isotherm, R is the universal gas constant, T is the system's temperature, and $55.5molL^{-1}$ is used as the unit of measure for the amount of water in a solution. For all of the measured isotherms, the computed value of ΔG_{ads} ranges from -8.959 to $-14.181kJmol^{-1}$, which is significantly less than the threshold value of $-40kJmol^{-1}$ needed for the mechanism of chemical adsorption [12–13]. Table 5 presents these values of ΔG_{ads}. Therefore, extract from *Sarcocephalus latifolius* leaves spontaneously adsorbs to the surface of alloy steel, in accordance with the physical adsorption mechanism [15].

Using the Arrhenius equation 7 and the transition state equation 8, the impact of temperature on the plant extract of *Sarcocephalus latifolius* adhering to the surface of alloy steel was assessed.

$$lnCR = lnA - \frac{E_a}{RT} \quad (7)$$

$$ln\frac{CR}{T} = ln\left(\frac{R}{NAh} + \frac{\Delta S_a}{RT}\right) - \frac{\Delta H_a}{RT} \quad (8)$$

Where CR is the alloy steel corrosion rate, A is the pre-exponential factor, E_a is the activation energy, R is the molar gas constant, T is absolute temperature, ΔH_a is the enthalpy change of adsorption, ΔS_a is the entropy change of adsorption, NA is Avogadro's constant, h is Plank's constant.

Figure 5 shows the results of plotting lnCR against 1/T using equation 7, with a slope of $-E_a/R$ and intercept of lnA. A slope of $\Delta H_a/R$ was discovered when plotting ln(CR/T) against 1/T from equation 8 as shown in Figure 6. The result of the expression was compared to the slope to arrive at ΔH_a, and the intercept of the plot, which was equal to $\ln(R/NAh+\Delta S_a/RT)$, to arrive at ΔS_a. Results shown in Table 6 indicate a decrease in E_a values with increasing plant extract concentration. This is a sign that alloy steel corrosion in 0.6M HCl is being delayed by the presence of

the plant extract [3, 5, 8]. Table 6 also shows the positive values of ΔH_a, which indicate endothermicity of the process, and negative values of ΔS_a, which indicate a reduction in entropy at the plant extract-metal surface. The inhibitory process is further qualified by these thermodynamic factors to follow the physical adsorption mechanism.

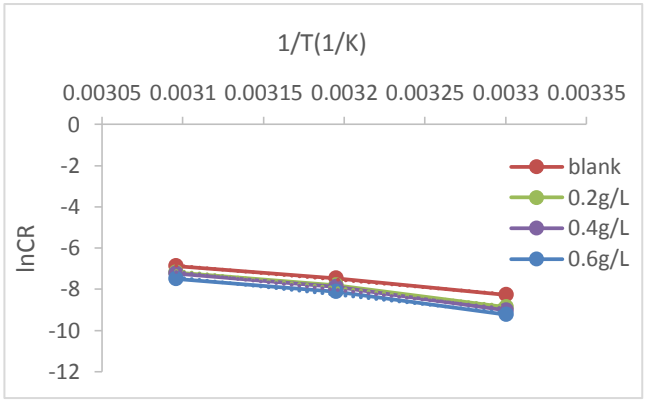

Fig 5. Arrhenius plot for inhibition of alloy steel using different concentrations of *Sarcocephalus latifolius* methanol leave extract in 0.6 M HCl

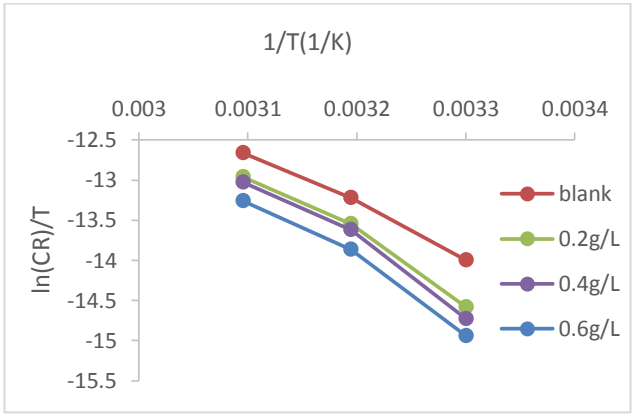

Fig 6. Transition state plot for the corrosion inhibition of alloy steel using different concentration of *Sarcocephalus latifolius* methanol extract in 0.6 M HCl.

Table 6. Energy parameters for the dissolution of alloy steel in 0.6M HCl in absence and presence of different concentrations of *Sarcocephalus latifolius* leave extract

Extract Conc. (g/L)	ΔH_a (kJ/mol)	E_a (kJ/mol)	ΔS_a (kJ/mol)
0.0	54.301	56.906	-0.1345
0.2	66.446	69.050	-0.0991
0.4	69.680	72.284	-0.0895
0.6	68.571	71.178	-0.0949

3.5 Kinetic Studies

By fitting the data from the weight loss experiment into various kinetic model equations, including zero, first, and second orders, the investigations of alloy steel corrosion in 0.6M HCl and its inhibition using the extract of *Sarcocephalus latifolius* were explored [24]. Equation 9–12 demonstrates how the first order kinetic equation, which was employed, was derived. The kinetic equation for the first order reaction is as reported in equation 9, where a_o is the initial weight of the alloy steel and x is the weight of the corrosion product lost after time (t) and k_1 is the rate constant of the reaction.

$$\frac{dx}{dt} = k_1(a_o - x) \quad (9)$$

Rearranging equation 9 produce equation 10 and upon integration of equation 10 yield equation 11-12 respectively. From the equations derived k_1 is the first order rate constant.

$$\frac{dx}{(a_o - x)} = k_1 dt \quad (10)$$

$$-ln(a_o - x) = k_1 t \quad (11)$$

$$-log\,(\Delta w) = k_1 \frac{t}{2.303} \quad (12)$$

Where $\Delta w = a_o - x$ is the weight loss of the alloy steel during corrosion.

The half-life equation was obtained by fitting the value of the k_1 constant into the half-life equation as shown in equation 13

$$t_{1/2} = \frac{0.693}{k_1} \quad (13)$$

The values of the kinetic parameters determined from the graphs were shown in Table 7 from the plot of -log(Δw) on the vertical axis against time, with t at the horizontal axis. Equation 14 was used to calculate the value of k_0 for the zero order kinetics models, while equation 15 was used to determine the relationship for the second order kinetics model. Equation 15 was used to display the graph of 1/w against time(t) and was used to derive the value of k_2 [24].

$$w_o = w + k_o t \quad (14)$$

$$\frac{1}{w} = \frac{1}{w_o} + k_2 t \quad (15)$$

Where w is weight loss at time t and w_o is the initial weight of the coupon metal, k_o and k_2 are the rate constants for zero and second order kinetics respectively.

Results reported in Table 7 revealed that the half-life values for the blank (0.6M HCl) ie uninhibited system were relatively lower than those for the inhibited medium which contained the plant extract with the immersed coupons of alloy steel. Additionally, it was revealed from the results that the half-life values increased proportionally with the increase in the plant extract concentration. By raising the values of their half-lives, this suggests that the methanol extract of *Sarcocephalus latifolius* functions as an inhibitor on alloy steel in the HCl medium [12]. The test results showed that the first order model best describes the process of the corrosion inhibition of the alloy steel in 0.6M HCl as carried out by the experiment when the values of the rate constants obtained were compared [12–14]. In comparison to other models evaluated, the R^2 values obtained for the

experiment were substantially closer to unity for the first order kinetic model [24–28].

Table 7. Kinetic parameters for the corrosion inhibition of alloy steel using *Sarcocephalus latifolius* extract in 0.6M HCl

Extract Conc. (g/L)	Zero Order R^2	k_0 (mol/Lhr^{-1})	$t_{1/2}$ (day)
0.0	0.625	0.0274	1.054
0.2	0.621	0.0175	1.650
0.4	0.569	0.0160	1.805
0.6	0.616	0.0176	1.641
Extract Conc.(g/L)	**First Order R^2**	**k_1 (hr^{-1})**	**$t_{1/2}$ (day)**
0.0	0.949	0.100	0.289
0.2	0.995	0.077	0.375
0.4	0.987	0.074	0.390
0.6	0.100	0.074	0.393
Extract Conc.(g/L)	**Second Order R^2**	**k_2 (mol/L)$^{-1}$**	**$t_{1/2}$ (day)**
0.0	0.699	0.0219	1.318
0.2	0.680	0.0162	1.783
0.4	0.813	0.0131	2.204
0.6	0.662	0.0107	2.699

4. Conclusion

In order to evaluate the corrosion inhibition of alloy steel in 0.6M HCl media at different temperatures, methanol leaves extract from *Sarcocephalus latifolius* was utilized. The research included surface characterization techniques like FT-IR and SEM as well as weight loss experiments.

- The weight loss experiment demonstrated that the plant extract's ability to inhibit corrosion of alloy steel in 0.6M HCl increases with concentration, while decreasing with increase in temperature.
- The highest value of the alloy steel inhibition was obtained at 0.6g/L plant extract and 303K, with a value of 61.18%.
- Through the presence of phytochemicals on the surface of the alloy steel metal, the surface characterization techniques used also supported the mechanism of the plant extract's adsorption on the surface of the metal.
- The corrosion inhibition process's thermodynamic properties show that the inhibition is feasible and spontaneous, and the isotherm model defines the mechanism as a physical adsorption process.
- The process' kinetics was found to be best described by first order kinetics, with values for the activation energy and half-life rising with increase in the concentration of plant extract.

Acknowledgements

The surface characterization examination of the alloy steel coupons was carried out by the staff of the Central Laboratory Complex at Bayero University in Kano, Nigeria, which is acknowledged by the authors.

Conflict of Interest

The authors declare that they have no conflict of interest.

References

1. Abdullahi A, Ameenullah A. Corrosion inhibition potentials of Strichnos spinosa L. on Aluminium in 0.9 M HCl medium: experimental and theoretical investigations. *Algerian Journal of Engineering and Technology*. 2020; 3:28-37. http://dx.doi.org/10.5281/zenodo.4402204
2. Ayuba AM, Abdullateef A. Investigating the corrosion inhibition potentials of Strichnos spinosa L. Extract on aluminium in 0.3 M hydrochloric acid solution. *Journal of Applied Science and Environmental Studies.* 2021; 4(1):4-11. https://doi.org/10.48393/IMIST.PRSM/jases-v4i1.24275.
3. Popoola LT, Aderibigbe TA, Lala MA. Mild Steel Corrosion Inhibition in Hydrochloric Acid Using Cocoa Pod Husk-Ficus exasperata: Extract Preparation Optimization and Characterization. *Iranian Journal of Chemistry and Chemical Engineering (IJCCE)*. 2022; 41(2):482-92. https://doi.org/10.30492/ijcce.2021.114540.3752
4. Beniken M, Driouch M, Sfaira M, Hammouti B, Ebn Touhami M, Mohsin M. Kinetic–thermodynamic properties of a polyacrylamide on corrosion inhibition for C-steel in 1.0 M HCl medium: part 2. *Journal of Bio-and Tribo-Corrosion*. 2018**;** 4(3):1-3. https://doi.org/10.1007/s40735-018-0152-1
5. Singh A, Ansari KR, Chauhan DS, Quraishi MA, Lgaz H, Chung IM. Comprehensive investigation of steel corrosion inhibition at macro/micro level by ecofriendly green corrosion inhibitor in 15% HCl medium. *Journal of colloid and interface science*. 2020; 560:225-236. https://doi.org/10.1016/j.jcis.2019.10.040
6. Zarrouk A, Zarrok H, Salghi R, Hammouti B, Bentiss F, Touir R, Bouachrine MO. Evaluation of N-containing organic compound as corrosion inhibitor for carbon steel in phosphoric acid. *J Mater Environ Sci*. 2013; 4(2):177-192.
7. Fazal BR, Becker T, Kinsella B, Lepkova K. A review of plant extracts as green corrosion inhibitors for CO2 corrosion of carbon steel. npj *Materials Degradation*. 2022; 6(1):1-4. https://doi.org/10.1038/s41529-021-00201-5
8. Li W, Zhang Z, Zhai Y, Ruan L, Zhang W, Wu L. Electrochemical and computational studies of proline and captopril as corrosion inhibitors on carbon steel in a phase change material solution. *Int. J. Electrochem. Sci*. 2020; 15(1):722-739. https://doi.org/10.20964/2020.01.63

9. Ekemini BI, Uwemedimo EU. Phytochemical profile, adsorptive and inhibitive of Costus afer extracts on aluminium corrosion in hydrochloric acid. *Research Library Der Chemica Sinica*, 2012, 3(6):1394-1405.
10. Rajamohan N, Al Shibli FS, Rajasimman M. Environmentally benign Prosopis juliflora extract for corrosion protection by sorption-Gravimetric, mechanistic and thermodynamic studies. *Environmental Research*. 2022; 203:111816. https://doi.org/10.1016/j.envres.2021.111816
11. Ayuba AM, Abubakar M. Inhibiting aluminium acid corrosion using leaves extract of Guiera senegalensis. *Journal of Fundamental and Applied Sciences*. 2021, 13(2):634-656. https://doi.org/10.4314/jfas.v13i2.1
12. Chahul HF, Ayuba AM, Nyior S. Adsorptive, Kinetic, Thermodynamic and Inhibitive Properties of Cissus Populnea Stem Extract on the Corrosion of Aluminum in Acid Medium. *ChemSearch Journal*. 2015; 6(1):20-30. http://dx.doi.org/10.4314/csj.v6i1.4
13. Abdullahi A, Muhammad A. DFT and molecular dynamic simulation study on the corrosion inhibition of Aluminum by some flavonoids of Guiera Senegalensis leaves. *Algerian Journal of Engineering and Technology*. 2021; 4:66-73. http://dx.doi.org/10.5281/zenodo.4636546
14. Husaini M, Usman B, Ibrahim MB. Study of corrosion inhibition performance of Glutaraldehyde on Aluminium in nitric acid solution. *Algerian Journal of Engineering and Technology*. 2020; 2:3-10 https://doi.org/10.5281/zendo.3923029
15. Wan S, Wei H, Quan R, Luo Z, Wang H, Liao B, Guo X. Soybean extract firstly used as a green corrosion inhibitor with high efficacy and yield for carbon steel in acidic medium. *Industrial Crops and Products*. 2022; 187:115354. https://doi.org/10.1016/j.indcrop.2022.115354
16. El Azzouzi M, Azzaoui K, Warad I, Hammouti B, Shityakov S, Sabbahi R, Saoiabi S, Youssoufi MH, Akartasse N, Jodeh S, Lamhamdi A. Moroccan, Mauritania, and senegalese gum Arabic variants as green corrosion inhibitors for mild steel in HCl: Weight loss, electrochemical, AFM and XPS studies. *Journal of Molecular Liquids*. 2022; 347:118354. https://doi.org/10.1016/j.molliq.2021.118354
17. Behera D, Nandi BK, Bhattacharya S. Variations in combustion properties of coal with average relative density and functional groups identified by FTIR analysis. *International Journal of Coal Preparation and Utilization*. 2022; 42(6):1695-1711. https://doi.org/10.1080/19392699.2020.1755661
18. Salman TA, Al-Azawi KF, Mohammed IM, Al-Baghdadi SB, Al-Amiery AA, Gaaz TS, Kadhum AA. Experimental studies on inhibition of mild steel corrosion by novel synthesized inhibitor complemented with quantum chemical calculations. *Results in Physics*. 2018; 10:291-296. https://doi.org/10.1016/j.rinp.2018.06.019
19. Eddy NO, Ameh PO, Essien NB. Experimental and computational chemistry studies on the inhibition of aluminium and mild steel in 0.1 M HCl by 3-nitrobenzoic acid. *Journal of Taibah University for Science*. 2018; 12(5):545-556. https://doi.org/10.1080/16583655.2018.1500514
20. de Vargas Brião G, da Silva MG, Vieira MG, Chu KH. Correlation of type II adsorption isotherms of water contaminants using modified BET equations. *Colloid and Interface Science Communications.* 2022; 46:100557. https://doi.org/10.1016/j.colcom.2021.100557
21. Umaru U, Ayuba AM. Quantum chemical calculations and molecular dynamic simulation studies on the corrosion inhibition of aluminium metal by myricetin derivatives. *Journal of New Technology and Materials*. 2020; 10:18-28.
22. Jyothi S, Rathidevi K. Experimental and theoretical investigation on corrosion inhibition of mild steel in sulphuric acid by coccinia indica leaves extract. *Rasāyan Journal of Chemistry*. 2017; 10(4):125312-60. http://dx.doi.org/10.7324/RJC.2017.1041924
23. Husaini M. Effect of Anisaldehyde as Corrosion Inhibitor for Aluminium in Sulphuric Acid Solution. *Journal of Science and* Technology. 2020; 12(2):1-10. https://doi.org/10.30880/jst. 2020.12.02.001
24. Ayuba AM, Uzairu A, Abba H, Shallangwa GA. Theoretical study of aspartic and glutamic acids as corrosion inhibitors on aluminium metal surface. *Moroccan Journal of Chemistry*. 2018; 6(1):160-172. https://doi.org/10.48317/IMIST.PRSM/morjchem-v6i1.9111
25. Hrimla M, Bahsis L, Boutouil A, Laamari MR, Julve M, Stiriba SE. A combined computational and experimental study on the mild steel corrosion inhibition in hydrochloric acid by new multifunctional phosphonic acid containing 1, 2, 3-triazoles. *Journal of Adhesion Science and Technology*. 2020; 34(16):1741-1773. https://doi.org/10.1080/01694243.2020.1728177.
26. Elmi S, Foroughi MM, Dehdab M, Shahidi-Zandi M. Computational evaluation of corrosion inhibition of four quinoline derivatives on carbon steel in aqueous phase. *Iranian Journal of Chemistry and Chemical Engineering (IJCCE)*. 2019; 38(1):185-200.
27. Lgaz H, Saha SK, Chaouiki A, Bhat KS, Salghi R, Banerjee P, Ali IH, Khan MI, Chung IM. Exploring the potential role of pyrazoline derivatives in corrosion inhibition of mild steel in hydrochloric acid solution: Insights from experimental and computational studies. *Construction and Building Materials*. 2020; 233:117320. https://doi.org/10.1016/j.conbuildmat.2019.117320.
28. Dagdag O, Safi Z, Erramli H, Cherkaoui O, Wazzan N, Guo L, Verma C, Ebenso EE, El Harfi A. Adsorption and anticorrosive behavior of aromatic epoxy monomers on carbon steel corrosion in acidic solution: computational studies and sustained experimental studies. *RSC advances*. 2019; 9(26):14782-14796 https://doi.org/10.1039/C9RA01672D.

Recommended Citation

Iorhuna F., Ayuba AM. Adsorptive, Kinetic and Thermodynamic Investigations of *Sarcocephalus latifolius* Leaves Extract as Corrosion Inhibitor on Alloy Steel in 0.6M HCl Solution. *Alger. J. Eng. Technol. 2022*; 7:83-91.

This work is licensed under a Creative Commons Attribution-NonCommercial 4.0 International License